

# Spin-orbit induced mixed-spin ground state in $R\text{NiO}_3$ perovskites probed by XAS: new insight into the metal to insulator transition

C. Piamonteze,<sup>1,2</sup> F. M. F. de Groot,<sup>3</sup> H. C. N. Tolentino,<sup>1</sup> A. Y. Ramos,<sup>1,4</sup> N. E. Massa,<sup>5</sup> J. A. Alonso,<sup>6</sup> and M. J. Martínez-Lope<sup>6</sup>

<sup>1</sup>Laboratório Nacional Luz Síncrotron, Caixa Postal 6192, 13084-971, Campinas/SP, Brazil

<sup>2</sup>IFGW/UNICAMP, 13083-970, Campinas/SP, Brazil

<sup>3</sup>Department of Inorganic Chemistry and Catalysis, Utrecht University, Sorbonnelaan 16, 3584 CA, Utrecht, The Netherlands

<sup>4</sup>LMCP - CNRS, Université de Paris 6, Paris, France

<sup>5</sup>Laboratorio Nacional de Investigación y Servicios en Espectroscopía Óptica, Centro CEQUINOR, UNLP, 1900 La Plata, Argentina

<sup>6</sup>Instituto de Ciencia de Materiales de Madrid, C.S.I.C., Cantoblanco, E-28049 Madrid, Spain  
(Dated: 2nd February 2008)

We report on a Ni  $L_{2,3}$  edges x-ray absorption spectroscopy (XAS) study in  $R\text{NiO}_3$  perovskites. These compounds exhibit a metal to insulator ( $MI$ ) transition as temperature decreases. The  $L_3$  edge presents a clear splitting in the insulating state, associated to a less hybridized ground state. Using charge transfer multiplet calculations, we establish the importance of the crystal field and 3d spin-orbit coupling to create a mixed-spin ground state. We explain the  $MI$  transition in  $R\text{NiO}_3$  perovskites in terms of modifications in the  $\text{Ni}^{3+}$  crystal field splitting that induces a spin transition from an essentially low-spin (LS) to a mixed-spin state.

PACS numbers: 61.10.Ht, 71.30.+h, 75.10.Dg, 75.25.+z

Keywords: x-ray absorption spectroscopy, XAS, metal-insulator transition, charge transfer multiplet theory

Rare-earth nickel perovskites ( $R\text{NiO}_3$ ,  $R$ =rare earth) present a sharp well-defined metal to insulator ( $MI$ ) transition as temperature decreases<sup>1</sup>. The transition temperature,  $T_{MI}$ , increases with reducing the  $R$  ion size, which determines the degree of distortion of the structure<sup>2</sup>. It was proposed that the gap opening would be due to a smaller Ni-O-Ni superexchange angle leading to a reduction of the bandwidth<sup>3</sup>. However, non-negligible electron-phonon interactions<sup>4</sup> and a shift in  $T_{MI}$  with oxygen isotope substitution<sup>5</sup> evidenced the importance of modifications in Ni-O interatomic distances, suggesting a phonon assisted mechanism for conduction. As temperature decreases, these nickelates undergo a magnetic transition to an unusual antiferromagnetic order<sup>6,7,8</sup>. The magnetic arrangement for the lighter  $R$  compounds ( $R$ =Pr, Nd, Sm, Eu) was refined with a single Ni moment ( $0.9\mu_B$ ) and required non-equivalent couplings among Ni ions to stabilize the structure<sup>6,7</sup>. This is a quite unusual situation in an orthorhombic crystallographic structure whose Ni sites are all equivalent<sup>2</sup>. For the heavier  $R$  compounds, Alonso *et al.*<sup>8,9</sup> established a monoclinic distortion in the crystallographic structure leading to two different Ni sites with longer and shorter Ni-O distances alternating along the three axis. The antiferromagnetic structure was explained by a charge ordering defined among the different Ni sites, each one with different magnetic moments ( $1.4$  and  $0.7\mu_B$  for  $\text{YNiO}_3$ )<sup>8</sup>. More recently, some evidences that the low temperature distortion is shared by all members of the  $R\text{NiO}_3$  family were reported<sup>10</sup>. Concerning the Ni local structure, our recent EXAFS results demonstrated the existence of two different Ni sites in all  $R\text{NiO}_3$  compounds, regardless their long-range crystallographic structure<sup>11,12</sup>.

From spectroscopic data together with configuration interaction calculations, Mizokawa *et al.*<sup>13</sup> established for  $\text{PrNiO}_3$  at room temperature a metallic ground state composed of  $34\%3d^7+56\%3d^8\bar{\mathbf{L}}+10\%3d^9\bar{\mathbf{L}}^2$ , where  $\bar{\mathbf{L}}$  stands for a ligand hole. Owing to the high degree of hybridization in the ground state, with hole-transfer from Ni3d to O2p orbitals, these compounds have been classified as self-doped Mott insulators<sup>14</sup>. Such a mixed metallic ground state, mostly  $3d^8\bar{\mathbf{L}}$ , is compatible with a  $\text{Ni}^{3+}$  low-spin configuration, because the amount of charge transfer for parallel spin almost equals that for antiparallel spin<sup>13</sup>. However, the spectral shape in  $R\text{NiO}_3$  compounds is very sensitive to the transition from metallic to insulating states<sup>15</sup> and a complete description of the spin degree of freedom remains to be given. As in recent outcomes on  $\text{Co}^{3+}$  oxides<sup>16,17</sup>, where unconventional spin states exist due to the competition between crystal field splitting and effective 3d exchange interaction, assignments made so far about  $\text{Ni}^{3+}$  in  $R\text{NiO}_3$  compounds have to be reexamined.

We report here Ni L-edge absorption measurements, which probes directly the available Ni3d states, together with charge transfer multiplet calculations. We establish the importance of the crystal field and 3d spin-orbit ( $l \cdot s$ ) coupling to create a mixed-spin ground state. We explain the  $MI$  transition in  $R\text{NiO}_3$  perovskites in terms of modifications in the  $\text{Ni}^{3+}$  crystal field splitting that localizes the electronic states and induces a spin transition from an essentially low-spin (LS) to a mixed-spin state, with a quite large contribution from a high-spin (HS) state.

Soft x-ray absorption measurements at the Ni  $L_{2,3}$  edges were carried out at the SGM beamline of LNLS, Brazil, using a spherical grating monochromator with an

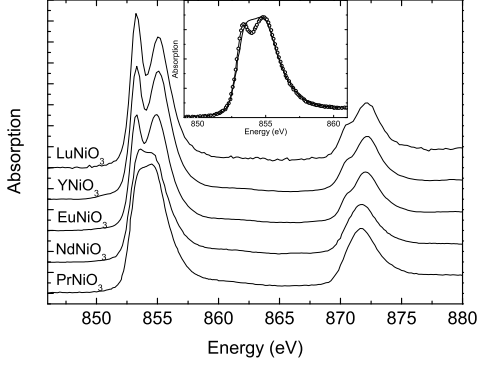


Figure 1: Ni  $L_{2,3}$  edge spectra at 300K for  $\text{PrNiO}_3$ ,  $\text{NdNiO}_3$ ,  $\text{EuNiO}_3$ ,  $\text{YNiO}_3$  and  $\text{LuNiO}_3$ , whose  $T_{MI}$  are 130, 200, 462, 582 and 599K, respectively. Inset:  $L_3$  edge spectra for  $\text{PrNiO}_3$  at 300K (solid line) and at 96K (open circles).

energy resolution of 0.8eV at 845eV. Data were collected at 300K and 96K using a liquid nitrogen cold finger. The bulk polycrystalline  $R\text{NiO}_3$  ( $R=\text{Pr}$ ,  $\text{Nd}$ ,  $\text{Eu}$ ,  $\text{Y}$  and  $\text{Lu}$ ) samples were obtained by a wet-chemistry technique, as described elsewhere<sup>18</sup>. The experimental spectra measured at 300K for  $\text{LuNiO}_3$ ,  $\text{YNiO}_3$ ,  $\text{EuNiO}_3$ ,  $\text{NdNiO}_3$  and  $\text{PrNiO}_3$  are shown in figure 1. The  $MI$  transition for these compounds takes place at 599K, 582K, 460K, 200K and 130K, respectively<sup>9</sup>. At 300K,  $\text{NdNiO}_3$  and  $\text{PrNiO}_3$  are at the metallic state whereas the other compounds are at the insulating state. For the insulators, a clear splitting is observed at the  $L_3$  edge ( $\sim 854\text{eV}$ ), while for the metals this splitting is absent. Differences among spectra measured in the different electronic states are also noticeable at the  $L_2$  edge ( $\sim 872\text{eV}$ ).  $\text{PrNiO}_3$  and  $\text{NdNiO}_3$  compounds spectra measured at 96K, when both are insulators, are analogous to those of  $R=\text{Eu}$ ,  $\text{Y}$  and  $\text{Lu}$  at 300K, as shown by the splitting at the  $L_3$  edge for the  $\text{PrNiO}_3$  compound (inset fig.1). Such modifications in the experimental spectra, unambiguously associated to the  $MI$  transition, demonstrate that important changes take place at the Ni local electronic structure. As the spectral shape depends mostly if the compound is metal or insulator, we conclude that the short range scale electronic structure of all compounds shares a common basis.

To identify the electronic interactions accounting for the experimental data, charge transfer (configuration interaction) multiplet (CTM)<sup>19,20</sup> calculations were carried out. The calculations take into account interactions between three configurations,  $3d^7$ ,  $3d^8\bar{\mathbf{L}}$ , and  $3d^9\bar{\mathbf{L}}^2$ , in  $D_{4h}$  symmetry. A series of calculations varying the crystal field splitting parameter  $10D_q$ , keeping  $D_s = 0.1\text{eV}$ ,  $D_t = 0.2\text{eV}$  fixed, is presented in figure 2. The configuration interaction parameters are  $\Delta = 0.5\text{eV}$ ,  $U_{dd} - U_{pd} = -1\text{eV}$  and the transfer integrals  $T(B_1) = T(A_1) = 2T(B_2) = 2T(E) = 2\text{eV}$ . The calculations matching the best with the experimen-

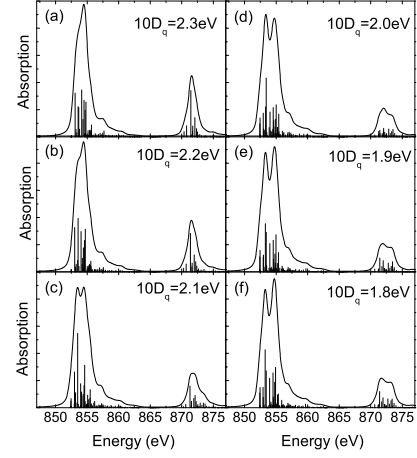


Figure 2: CTM calculations of the Ni L XAS spectra in  $D_{4h}$  symmetry. The value of  $10D_q$  is varied between 2.3 eV (a) and 1.8 eV (f), in steps of 0.1 eV. The other parameters used are described in the text.

tal spectra for the metallic compounds are those with  $10D_q = 2.2\text{eV}$ . The  $\text{Ni}^{3+}$  metallic ground state turns out to be composed of  $49\%3d^7 + 47\%3d^8\bar{\mathbf{L}} + 4\%3d^9\bar{\mathbf{L}}^2$ . The relative proportions for the three configurations are in reasonable agreement with those found by Mizokawa *et al.* for metallic  $\text{PrNiO}_3$ <sup>13</sup>. The slight difference can be partially ascribed to the way the ligand hole is treated in the codes<sup>21</sup>. For the insulating compounds, a very good agreement with experiments is achieved by decreasing  $10D_q$  down to 2.0 or 1.9eV. Such a decrease in  $10D_q$  leads to a less hybridized ground state composed of  $61\%3d^7 + 37\%3d^8\bar{\mathbf{L}} + 2\%3d^9\bar{\mathbf{L}}^2$ .

Figure 3a shows the simulated spectrum for  $10D_q = 1.9\text{eV}$  taking into account the  $l \cdot s$  coupling, as in fig.2e, while figure 3b shows the calculation without  $l \cdot s$  coupling. The effect on the spectral shape is remarkable. The ground state without  $l \cdot s$  coupling is a HS state, schematically represented in figure 3d. Figure 3c shows a calculation without  $l \cdot s$  coupling, but when the initial state of the transition is the first excited state, which is a LS state, schematically represented in figure 3e. The energy difference between these two states is found to be  $\sim 0.1\text{eV}$ . Since the  $l \cdot s$  coupling is of the same order, the insulating ground state turns out to be a mixing of LS and HS states. In addition, the calculation of the metallic state (fig.2b) is quite similar to that shown in fig.3c, indicating that the LS state gives the main contribution to the metallic ground state. We conclude that the ground state composition is very sensitive to the spin-orbit ( $l \cdot s$ ) coupling and that modifications in the crystal field splitting ( $10D_q$ ) change the relative contribution of both states to the mixed ground state.

The ground state (GS) can be decomposed into different symmetries that are mixed up by the  $l \cdot s$  coupling:

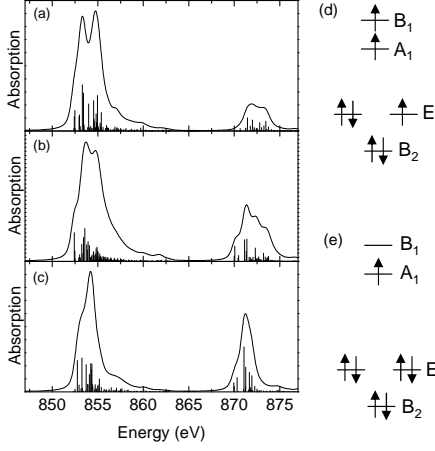


Figure 3: CTM calculations for  $10D_q = 1.9\text{eV}$  (a) with  $l \cdot s$  coupling, (b) without  $l \cdot s$  coupling and (c) without  $l \cdot s$  coupling but with the initial state being the first excited state; (d) Scheme of HS -  $^4E$  and (e) LS -  $^2A_1$  states.

$$\begin{aligned} \Psi_{GS} = & \sum_{i; k+l+m+n=3} \alpha_i |a_1^k b_1^l b_2^m e^n\rangle \\ & + \sum_{j; k'+l'+m'+n'=2} \alpha_j |a_1^{k'} b_1^{l'} b_2^{m'} e^{n'} \underline{\mathbf{L}}\rangle \\ & + \sum_{p; k''+l''+m''+n''=1} \alpha_p |a_1^{k''} b_1^{l''} b_2^{m''} e^{n''} \underline{\mathbf{L}}^2\rangle \quad (1) \end{aligned}$$

In this expression  $k + l + m + n$ ,  $k' + l' + m' + n'$  and  $k'' + l'' + m'' + n''$  are the number of d holes in  $3d^7$ ,  $3d^8 \underline{\mathbf{L}}$  and  $3d^9 \underline{\mathbf{L}}^2$  configurations, respectively. The  $\alpha_i$ ,  $\alpha_j$ ,  $\alpha_p$  values can be obtained as described by Wasinger *et al.*<sup>22</sup>. The contributions of these different symmetries to the ground state and to spin ( $S_z$ ) and orbital angular ( $L_z$ ) moments as function of  $10D_q$  are shown in figure 4. The labels in figure 4b refer to the distribution of the d holes among  $B_1$ ,  $A_1$ ,  $B_2$  and  $E$  orbitals. At the metallic state, with  $10D_q = 2.2\text{eV}$ , the ground state is composed of  $\sim 38\%$   $\underline{B_1 B_1 A_1}$  (LS) and a small amount ( $\sim 8\%$ ) of  $\underline{B_1 A_1 E}$  (HS), the rest being charge transfer configurations. This leads to a net spin moment  $S_z \sim 0.5$ , in accordance with previous results that found a LS state for the metallic  $\text{PrNiO}_3$ <sup>13</sup>. Despite of this strongly hybridized ground state, the expected value for  $S_z$  is close to the  $\text{Ni}^{3+}$  LS ionic value. The reason is essentially due to the charge transfer configurations. The amount of charge transfer with spin up ( $S_z = 1$  from  $\underline{B_1 A_1 \underline{L}}$ ) is compensated by that of spin down ( $S_z = 0$  from  $\underline{B_1 B_1 \underline{L}}$ ). The ground state transition takes place at  $10D_q = 2.1\text{eV}$ , where we obtain the same contributions for HS and LS states, that is, the ground state is made of  $\sim 25\%$   $\underline{B_1 A_1 E}$  and of  $\sim 25\%$   $\underline{B_1 B_1 A_1}$ . The spin moment assumes an intermediate value  $S_z \sim 0.7$ . At the insulating state, with  $10D_q = 2.0\text{eV}$ , the ground state is composed of  $\sim 46\%$

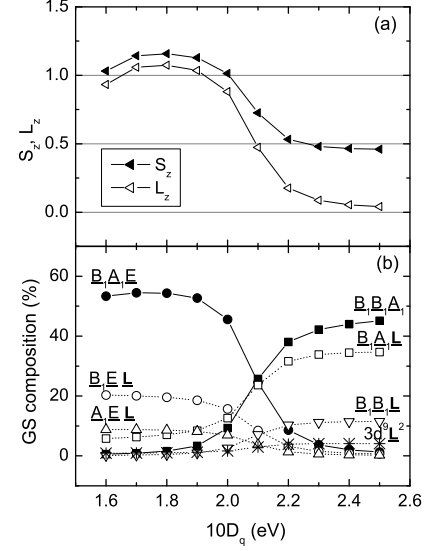


Figure 4: (a) Variation of  $S_z$ ,  $L_z$  and (b) ground state composition as a function of  $10D_q$ . The configuration  $\underline{B_1 B_1 A_1}$  corresponds to the LS  $^2A_1$  state in fig.3e and the configuration  $\underline{B_1 A_1 E}$  corresponds to the HS  $^4E$  state in fig.3d. The others correspond to charge transfer configurations.

$\underline{B_1 A_1 E}$  (HS) and a small amount ( $\sim 9\%$ ) of  $\underline{B_1 B_1 A_1}$  (LS), the complement coming from charge transfer configurations. This leads to a net spin moment  $S_z \sim 1.0$ . The mixed-spin state arises because these compounds are between the strong and weak field limit and also due to the strong hybridization that mixes the Ni3d and O2p orbitals. In case there would be no charge transfer at all, the high-spin to low-spin transition would take place over a crystal field range of less than 0.1 eV. So, it is due to the strong covalence that there is a gradual change from high-spin to low-spin ground state.

For the  $\underline{B_1 B_1 A_1}$  (LS) state, the electron coming from the O2p ligand band occupies the  $B_1$  orbital, even though it has a higher energy than  $A_1$ , owing to the gain in exchange energy. So,  $\underline{B_1 A_1 \underline{L}}$  is the most important charge transfer configuration at the metallic state. On the other hand, for the  $\underline{B_1 A_1 E}$  (HS) state, the ligand electron must occupy an orbital already filled and there is no gain in exchange energy. In this case, the ligand electron occupies the  $A_1$  orbital, which is lower in energy than  $B_1$  and has a transfer integral twice larger than for the  $E$  orbital. Moreover, the  $\underline{B_1 B_1 A_1}$  (LS) state has all its three holes in orbitals that have strong mixing with the O2p ligand band ( $A_1$  and  $B_1$  come from the  $e_g$  orbital in  $O_h$  symmetry), whereas the  $\underline{B_1 A_1 E}$  (HS) state has a more localized hole in an  $E$  orbital that has less efficient overlap with the O2p ligand band. So, the increase of the HS component in the ground state and the decrease of the hybridization for smaller  $10D_q$  are related to each other.

The physical reason for a smaller  $10D_q$  at the insulat-

ing state originates in the coexistence of two nonequivalent Ni sites and overall increase of the average Ni-O bonding in all  $R\text{NiO}_3$  compounds<sup>2,8,9</sup>. Nonequivalent Ni sites coexist even at the metallic state<sup>11,12</sup> and are compatible with a segregation into two phases, where a more localized electron phase is embedded in a conducting background<sup>23</sup>. The  $MI$  transition takes place with the increase of the less hybridized phase related to the other. Alonso *et al.*<sup>8</sup> found for the heavier  $R\text{NiO}_3$  compounds, by refining neutron diffraction data in the monoclinic symmetry, an antiferromagnetic structure compatible with two nonequivalent moments. The smaller and larger Ni sites display magnetic moments of 0.7 and  $1.4\mu_B$ , respectively. The values that we predict here for  $S_z$  are larger because the spin moment of the 3d elements retain most of their isolated ion properties in x-ray absorption spectroscopy. Owing to the short time scale in XAS essentially all electrons appear localized. Delocalized electrons should reduce these values in the solid. The same argument holds for the angular moment  $L_z$ , which is normally quenched in these compounds. Even if somewhat overestimated, our predictions show that an important parameter controlling the properties of these compounds is the small splitting in distances, which leads to a different crystal field in each site. For the lighter  $R\text{NiO}_3$  powder compounds, the long range structure has always been refined using a single Ni site and for that reason no such different spin values have been found. Recently, a monoclinic distortion was observed in thin films

of  $\text{NdNiO}_3$ <sup>24</sup>, questioning the orthorhombic symmetry obtained previously by neutrons. Our results show that the lighter and heavier  $R\text{NiO}_3$  compounds are very similar from the point of view of the local electronic structure. Experimental spectra look very similar and depend only if the compound is insulator or metal. So, we believe that the same physics observed in the heavier  $R\text{NiO}_3$  compounds may be involved in the lighter ones.

In conclusion, we presented experimental evidences of significant changes in the local electronic structure around  $\text{Ni}^{3+}$  in  $R\text{NiO}_3$  compounds. With the support of charge transfer multiplet calculations, we showed that, concomitantly with the metal to insulator transition, a decrease of the crystal field splitting leads to a ground state transition from an essentially LS to a mixed-spin ground state. The mixed-spin ground state is possible because the energy separation between HS and LS states is of the same order of the spin-orbit coupling. The smaller hybridization, intrinsic to the HS state, gives an explanation to the more localized character at the insulating regime. The existence of a mixed-spin state, involving both LS and HS states and also charge transfer configurations, shed new light in the understanding of the unusual antiferromagnetic order observed below  $T_N$ , which is still an open question.

Work partially supported by LNLS/ABTLuS. CP thanks FAPESP for the PhD grant. AYR thanks CNPq for the visiting scientist grant.

- 
- <sup>1</sup> P. Lacorre, J. B. Torrance, J. Pannetier, A. I. Nazzal, P. W. Wang, and T. C. Huang, *J. Solid State Chem.* **91**, 225 (1991).
  - <sup>2</sup> J. L. García-Muñoz, J. Rodríguez-Carvajal, P. Lacorre, and J. B. Torrance, *Phys. Rev. B* **46**, 4414 (1992).
  - <sup>3</sup> J. B. Torrance, P. Lacorre, A. I. Nazzal, E. J. Ansaldo, and C. Niedermayer, *Phys. Rev. B* **45**, 8209 (1992).
  - <sup>4</sup> N. E. Massa, J. A. Alonso, M. J. Martínez-Lope, and I. Rasines, *Phys. Rev. B* **56**, 986 (1997).
  - <sup>5</sup> M. Medarde, P. Lacorre, K. Conder, F. Fauth, and A. Furrer, *Phys. Rev. Lett.* **80**, 2397 (1998).
  - <sup>6</sup> J. L. García-Muñoz, J. Rodríguez-Carvajal, and P. Lacorre, *Phys. Rev. B* **50**, 978 (1994).
  - <sup>7</sup> J. Rodríguez-Carvajal, S. Rosenkranz, M. Medarde, P. Lacorre, M. T. Fernández-Díaz, F. Fauth, and V. Trounov, *Phys. Rev. B* **57**, 456 (1998).
  - <sup>8</sup> J. A. Alonso, J. L. García-Muñoz, M. T. Fernández-Díaz, M. A. G. Aranda, M. J. Martínez-Lope, and M. T. Casais, *Phys. Rev. Lett.* **82**, 3871 (1999).
  - <sup>9</sup> J. A. Alonso, M. J. Martínez-Lope, M. T. Casais, J. L. García-Muñoz, and M. T. Fernández-Díaz, *Phys. Rev. B* **61**, 1756 (2000).
  - <sup>10</sup> F. de la Cruz, C. Piamonteze, N. E. Massa, H. Salva, J. A. Alonso, M. J. Martínez-Lope, and M. T. Casais, *Phys. Rev. B* **66**, 153104 (2002).
  - <sup>11</sup> C. Piamonteze, H. C. Tolentino, A. Y. Ramos, N. E. Massa, J. A. Alonso, M. J. Martínez-Lope, and M. T. Casais, *physica Scripta*, in press.
  - <sup>12</sup> C. Piamonteze, H. C. Tolentino, A. Y. Ramos, N. E. Massa, J. A. Alonso, M. J. Martínez-Lope, and M. T. Casais, accepted to *Phys. Rev. B*
  - <sup>13</sup> T. Mizokawa, A. Fujimori, T. Arima, Y. Tokura, N. Mōri, and J. Akimitsu, *Phys. Rev. B* **52**, 13865 (1995).
  - <sup>14</sup> T. Mizokawa, D. I. Khomskii, and G. A. Sawatzky, *Phys. Rev. B* **61**, 11263 (2000).
  - <sup>15</sup> C. Piamonteze, H. C. Tolentino, F. C. Vicentin, A. Y. Ramos, N. E. Massa, J. A. Alonso, M. J. Martínez-Lope, and M. T. Casais, *Surf. Rev. Lett.* **9**, 1121 (2002).
  - <sup>16</sup> Z. Hu et al., *Phys. Rev. Lett.* **92**, 207402 (2004).
  - <sup>17</sup> I. A. Nekrasov et al., *Phys. Rev. B* **68**, 235113 (2003).
  - <sup>18</sup> J. A. Alonso, M. J. Martínez-Lope, and I. Rasines, *J. Solid State Chem.* **120**, 170 (1995).
  - <sup>19</sup> F. M. F. de Groot, *J. Electron Spectrosc. Relat. Phenom.* **67**, 529 (1994).
  - <sup>20</sup> F. M. F. de Groot, *Coor. Chem. Rev.* (2004).
  - <sup>21</sup> *The multiplet program used considers the ligand hole as having d symmetry, whereas, cluster programs take into account the real p-ligand states.*
  - <sup>22</sup> E. C. Wasinger, F. M. F. de Groot, B. Hedman, K. O. Hodgson, and E. I. Solomon, *J. Am. Chem. Soc.* **125**, 12894 (2003).
  - <sup>23</sup> J.-S. Zhou, J. B. Goodenough, B. Dabrowski, P. W. Klamut, and Z. Bukowski, *Phys. Rev. B* **61**, 4401 (2000).
  - <sup>24</sup> U. Staub, G. I. Meijer, F. Fauth, R. Allenspach, J. G. Bednorz, J. Karpinski, and S. M. Kazadov, *Phys. Rev. Lett.* **88**, 126402 (2002).